

ENERGY-SAVING CELL-FREE MASSIVE MIMO PRECODERS WITH A PER-AP WIDEBAND KRONECKER CHANNEL MODEL

Emanuele Peschiera* Xavier Mestre† François Rottenberg*

* Katholieke Universiteit Leuven, Ghent, Belgium

† Centre Tecnològic de Telecomunicacions de Catalunya, Barcelona, Spain

ABSTRACT

We study cell-free massive multiple-input multiple-output precoders that minimize the power consumed by the power amplifiers subject to per-user per-subcarrier rate constraints. The power at each antenna is generally retrieved by solving a fixed-point equation that depends on the instantaneous channel coefficients. Using random matrix theory, we retrieve each antenna power as the solution to a fixed-point equation that depends only on the second-order statistics of the channel. Numerical simulations prove the accuracy of our asymptotic approximation and show how a subset of access points should be turned off to save power consumption, while all the antennas of the active access points are utilized with uniform power across them. This mechanism allows to save consumed power up to a factor of $9\times$ in low-load scenarios.

Index Terms— Cell-Free Massive MIMO, Precoding, Random Matrix Theory, Power Amplifiers, Power Consumption.

1. INTRODUCTION

Energy-saving mechanisms are becoming increasingly present in wireless systems [1–3]. In the space domain, energy-saving strategies dynamically activate hardware resources, such as antennas and their radio frequency (RF) chains, or even entire access points (APs), as a function of the network load. Studies on cellular massive multiple-input multiple-output (MIMO) reveal that the traffic-aware (de)activation of hardware resources is a direct consequence of considering the consumed power instead of the transmit power, as conventionally done in the precoding design [4–6]. From the perspective of the power amplifiers (PAs) consumption, in a single-carrier system it is more convenient to saturate a subset of PAs, which can work at maximal efficiency, and switch off the remaining ones [4]. Considering the base station (BS) consumption, significant savings can be achieved by turning off some antennas and their associated RF chains [2].

In this work, we study the optimal precoding and power allocation, in terms of PAs consumption, for a cell-free massive MIMO (CF-mMIMO) network, where several distributed APs jointly serve the users [7]. This type of MIMO architecture offers substantial advantages towards sixth-generation (6G) systems thanks to its high network coverage and macro-diversity gain [8]. Studies in the literature have addressed the problem of switching on/off APs to minimize consumption [9–11], but in most cases, they rely on conventional precoders and optimize the power allocations according to the power consumption. Moreover, the impact of a multicarrier transmission is often overlooked. In this work, we formulate the precod-

ing problem as a minimization of the power consumed by the PAs under per-subcarrier zero-forcing (ZF) constraints. In the case of centralized processing, the problem is equivalent to the cellular one in [6], with the crucial difference being the channel model, which incorporates the characteristics of a CF-mMIMO scenario. The spatial distribution of the APs implies a channel having a different covariance matrix for each AP.

Despite its advantages, the large dimension of a complete CF-mMIMO observation can easily lead to significant growth in the power consumed by (i) the fronthaul links, (ii) the baseband processing at the central unit (CU), and (iii) the RF circuitry and power supply of all the APs. For this reason, leveraging random matrix theory (RMT) and the structure of the precoding solution, we derive simplified solutions to the addressed problem. The CU determines which APs to activate prior to computing the precoding matrices, and the set of active APs changes only with the second-order channel statistics. It can be shown that the proposed solution approaches the optimal one when the number of subcarriers increases (referred to as wideband regime since we consider a fixed subcarrier spacing).

2. SYSTEM MODEL

2.1. Signal Model

We consider the downlink of an orthogonal frequency-division multiplexing (OFDM) CF-mMIMO system with L APs, where AP l is equipped with M_l antennas, K single-antenna users and Q subcarriers. We consider fully-centralized processing, where all APs are connected to a CU. Moreover, all the active APs serve all the users. The total number of antennas in the system is $\sum_{l=0}^{L-1} M_l = N$. We group the signals relative to an AP in a contiguous manner. After precoding, the transmitted signal by all APs at subcarrier q is

$$\mathbf{x}_q = \left[\mathbf{x}_{0,q}^T, \dots, \mathbf{x}_{L-1,q}^T \right]^T = \mathbf{W}_q \mathbf{s}_q \in \mathbb{C}^{N \times 1} \quad (1)$$

where $\mathbf{x}_{l,q} \in \mathbb{C}^{M_l \times 1}$ is the transmitted signal by AP l at subcarrier q , $\mathbf{s}_q \in \mathbb{C}^{K \times 1}$ is the symbol vector at subcarrier q , and $\mathbf{W}_q \in \mathbb{C}^{N \times K}$ is the aggregated precoding matrix corresponding to all the APs at subcarrier q . We assume that $\mathbb{E} \{ \mathbf{s}_q \mathbf{s}_q^H \} = \mathbf{I}_K \forall q$. The received signal vector at subcarrier q is

$$\mathbf{r}_q = \mathbf{H}_q \mathbf{x}_q + \boldsymbol{\nu}_q \in \mathbb{C}^{K \times 1} \quad (2)$$

where $\mathbf{H}_q = [\mathbf{H}_{0,q}, \dots, \mathbf{H}_{L-1,q}] \in \mathbb{C}^{K \times N}$ is the aggregated channel matrix at subcarrier q , with $\mathbf{H}_{l,q} \in \mathbb{C}^{K \times M_l}$ being the channel matrix of AP l at subcarrier q , and $\boldsymbol{\nu}_q \sim \mathcal{CN}(\mathbf{0}_K, \sigma_\nu^2 \mathbf{I}_K)$ is the additive noise.

This work has been partially funded by a short-term scientific mission (STSM) grant from the COST ACTION CA20120 INTERACT.

2.2. Channel Model

We model the channel of the l th AP as

$$\mathbf{H}_{l,q} = \mathbf{D}_{\beta,l}^{\frac{1}{2}} \mathbf{G}_{l,q} \mathbf{C}_{\text{AP},l}^{\frac{1}{2}} \quad (3)$$

where $\mathbf{D}_{\beta,l} = \text{diag}(\beta_{0,l}, \dots, \beta_{K-1,l})$ is a diagonal matrix collecting the large-scale fading (LSF) coefficients for AP l , $\beta_{k,l} > 0$ is the LSF coefficient between user k and AP l , $\mathbf{G}_{l,q}$ models the small-scale fading and has independently and identically distributed (i.i.d.) entries drawn from a $\mathcal{CN}(0, 1)$ distribution, and $\mathbf{C}_{\text{AP},l} \in \mathbb{C}^{M_l \times M_l}$ expresses the correlation among the antennas of AP l . The above is equivalent to considering a per-AP Kronecker channel model, while \mathbf{H}_q follows a Weichselberger channel model [12].

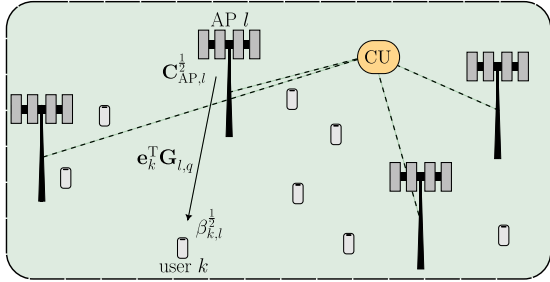


Fig. 1. Considered CF-mMIMO scenario.

2.3. Power Consumption Model

Given that we consider the transmitted symbols to be of unit variance and uncorrelated among subcarriers and users, the transmit power at antenna n is given by $p_n = \sum_{q=0}^{Q-1} \mathbf{e}_n^T \mathbf{W}_q \mathbf{W}_q^H \mathbf{e}_n$, where \mathbf{e}_n is the n th canonical basis vector of \mathbb{R}^N , thus the total transmit power is

$$P_{\text{tx}} = \sum_{q=0}^{Q-1} \text{tr} \mathbf{W}_q \mathbf{W}_q^H \quad (4)$$

where $\text{tr} \cdot$ is the trace operator. Under the PA consumption model in [4, 6], the total power consumed by the PAs is

$$P_{\text{PAs}} = \frac{p_{\text{max}}}{\eta_{\text{max}}} \sum_{n=0}^{N-1} \left(\sum_{q=0}^{Q-1} \mathbf{e}_n^T \mathbf{W}_q \mathbf{W}_q^H \mathbf{e}_n \right)^{\frac{1}{2}} \quad (5)$$

where p_{max} and η_{max} are the maximal PA transmit power and efficiency, respectively. The solutions that optimize (5) typically activate only part of the L APs. Let us therefore identify the set of the active APs of the optimum solution as $\mathcal{L}_a \subseteq \{0, \dots, L-1\}$, where the number of active APs is $|\mathcal{L}_a| = L_a$. To quantify the consumed power at the network level, we use the following model

$$P_{\text{net}} = P_{\text{PAs}} + \sum_{l \in \mathcal{L}_a} (P_{\text{fix}} + P_c M_{a,l}) \quad (6)$$

where P_{fix} is the fixed consumption associated with the activation of an entire AP, P_c is the cost (in terms of circuit power consumption) to activate a single antenna, and $M_{a,l}$ is the number of active antennas at AP l .

3. PRECODER DESIGN

As a benchmark, we consider the conventional ZF precoder, which solves

$$(\mathcal{P}_1): \min_{\{\mathbf{W}_q\}} P_{\text{tx}} \quad \text{s.t.} \quad \mathbf{H}_q \mathbf{W}_q = \tilde{\mathbf{D}}_{\gamma}^{\frac{1}{2}} \sigma_{\nu} \quad \forall q \quad (7)$$

where $\tilde{\mathbf{D}}_{\gamma} = \frac{1}{Q} \text{diag}(\gamma_0, \dots, \gamma_{K-1})$, γ_k being the target signal-to-noise ratio (SNR) of user k , and σ_{ν}^2 is the noise power. The ZF constraints can be easily translated into rate constraints, e.g., an achievable rate for user k at subcarrier q is $\log_2(1 + \frac{\gamma_k}{Q})$ bits per channel use. The solution to (\mathcal{P}_1) is the per-subcarrier ZF

$$\mathbf{W}_q = \mathbf{H}_q^H \left(\mathbf{H}_q \mathbf{H}_q^H \right)^{-1} \tilde{\mathbf{D}}_{\gamma}^{\frac{1}{2}} \sigma_{\nu}. \quad (8)$$

We are instead interested in the precoder that minimizes the power consumed by the PAs under a ZF constraint, corresponding to

$$(\mathcal{P}_2): \min_{\{\mathbf{W}_q\}} P_{\text{PAs}} \quad \text{s.t.} \quad \mathbf{H}_q \mathbf{W}_q = \tilde{\mathbf{D}}_{\gamma}^{\frac{1}{2}} \sigma_{\nu} \quad \forall q. \quad (9)$$

Let us define $\tilde{\mathbf{H}}_q = \sigma_{\nu}^{-1} \tilde{\mathbf{D}}_{\gamma}^{-\frac{1}{2}} \mathbf{H}_q$ as the normalized channel matrix.

Proposition 1. *The solution to (\mathcal{P}_2) has the following form [6]*

$$\bar{\mathbf{W}}_q = \mathbf{D}_{\mathbf{p}}^{\frac{1}{2}} \mathbf{H}_q^H \left(\mathbf{H}_q \mathbf{D}_{\mathbf{p}}^{\frac{1}{2}} \mathbf{H}_q^H \right)^{-1} \tilde{\mathbf{D}}_{\gamma}^{\frac{1}{2}} \sigma_{\nu} \quad (10)$$

where $\mathbf{D}_{\mathbf{p}} = \text{diag}(p_0, \dots, p_{N-1})$ contains the powers transmitted by the antennas. The transmit power at antenna n can be written as the solution to the set of equations (for $n = 1, \dots, N$)

$$p_n = \sum_{q=0}^{Q-1} \mathbf{e}_n^T \mathbf{D}_{\mathbf{p}}^{\frac{1}{2}} \tilde{\mathbf{H}}_q^H \left(\tilde{\mathbf{H}}_q \mathbf{D}_{\mathbf{p}}^{\frac{1}{2}} \tilde{\mathbf{H}}_q^H \right)^{-2} \tilde{\mathbf{H}}_q \mathbf{D}_{\mathbf{p}}^{\frac{1}{2}} \mathbf{e}_n \quad (11)$$

which can be retrieved via iterative fixed-point algorithm.

The structure of the precoder in (10) allows one to allocate more power to some antennas, which can work closer to the PA saturation level. Turning off some antennas/APs implies further savings in P_{net} . Note that the CU needs to (i) compute the antenna powers in (11) every time the small-scale fading changes (i.e., every channel coherence time) and (ii) know the instantaneous channel coefficients of all the APs, which corresponds to NKQ elements. These operations impose challenging requirements to the fronthaul capacity of a CF-mMIMO system due to the large number of antennas/APs. For this reason we propose, in the next section, a RMT approach that reduces the complexity of retrieving the APs powers.

4. ASYMPTOTIC ANALYSIS

In this section, we consider the following asymptotic regime.

(As1): $M_l \rightarrow \infty \forall l \in \{0, \dots, L-1\}$ and $K \rightarrow \infty$. Moreover, defining $c_l = \frac{K}{M_l}$, there exist $b > a > 0$ for which $a < \min_l \liminf_K c_l < \max_l \limsup_K c_l < b$.

Thanks to the hardening effect that happens in this regime, the random quantities in (11) behave as deterministic ones [13]. Nonetheless, the solution to the system of equations in (11) has N components, therefore **(As1)** implies that the dimension of the solution grows infinitely large. The number of APs L is instead fixed. This motivates the introduction of the following assumption.

(As2): $\mathbf{D}_p = \text{blkdiag} \left(\{p_l \mathbf{I}_{M_l}\}_{l=0}^{L-1} \right)$, where $\text{blkdiag}(\cdot)$ is the block-diagonal operator, corresponding to a uniform power allocation per AP. Therefore, the effective dimension of the solution is fixed and equal to L .

The above assumption is an approximation, indeed one can retrieve the exact solution to (11) and observe that more power is allocated to the least correlated antennas. However, numerical simulations will demonstrate that the results obtained under (As2) have a negligible performance loss compared to the optimal ones. The following assumptions are also made.

(As3): $\forall l \in \{0, \dots, L-1\}$, $\mathbf{G}_{l,q} \in \mathbb{C}^{K \times M_l}$ has i.i.d. entries with zero mean and unit variance.

(As4): $\forall l \in \{0, \dots, L-1\}$, $\mathbf{D}_l \in \mathbb{R}^{K \times K}$, $\mathbf{C}_{\text{AP},l} \in \mathbb{C}^{M_l \times M_l}$ and $\mathbf{D}_p \in \mathbb{R}^{N \times N}$ are deterministic matrices with bounded spectral norms. Moreover, \mathbf{D}_p has at least $K+1$ non-zero entries.

While in the previous section we did not rely on any specific channel model, we now consider the per-AP Kronecker channel in (3). By defining $\mathbf{D}_l = \sigma_\nu^{-2} \tilde{\mathbf{D}}_\gamma^{-1} \mathbf{D}_{\beta,l}$, we can write

$$\tilde{\mathbf{H}}_q \mathbf{D}_p^{\frac{1}{2}} \tilde{\mathbf{H}}_q^H = \sum_{l=0}^{L-1} p_l^{\frac{1}{4}} \mathbf{D}_l^{\frac{1}{2}} \mathbf{G}_{q,l} \mathbf{C}_{\text{AP},l} \mathbf{G}_{q,l}^H \mathbf{D}_l^{\frac{1}{2}} p_l^{\frac{1}{4}}. \quad (12)$$

The above model is analyzed by the authors in [14]. In our case, we want to characterize $\mathbf{e}_n^T \mathbf{D}_p^{\frac{1}{2}} \tilde{\mathbf{H}}_q \left(\tilde{\mathbf{H}}_q \mathbf{D}_p^{\frac{1}{2}} \tilde{\mathbf{H}}_q^H \right)^{-2} \tilde{\mathbf{H}}_q \mathbf{D}_p^{\frac{1}{2}} \mathbf{e}_n$, which corresponds to the left-hand side of (11). It turns out that this quantity is asymptotically equivalent to a deterministic one (almost surely) as the system dimensions increase to infinity. Let us now introduce the variables b_l , $l \in \{0, \dots, L-1\}$, which form the unique non-negative solutions to the L equations

$$b_l = \frac{1}{K} \text{tr} p_l^{\frac{1}{2}} \mathbf{D}_l \left(\sum_{l'=0}^{L-1} \frac{1}{M_{l'}} \sum_{m=0}^{M_{l'}-1} \frac{\xi_{l',m}}{1 + c_{l'} \xi_{l',m} b_{l'}} p_{l'}^{\frac{1}{2}} \mathbf{D}_{l'} \right)^{-1} \quad (13)$$

where $\xi_{l,m}$ is the m th eigenvalue of $\mathbf{C}_{\text{AP},l}$. The variables b_l , $l \in \{0, \dots, L-1\}$, are defined as

$$\begin{bmatrix} b_0 \\ \vdots \\ b_{L-1} \end{bmatrix} = (\mathbf{I}_L - \mathbf{A})^{-1} \begin{bmatrix} \frac{1}{K} \text{tr} p_0^{\frac{1}{2}} \mathbf{D}_0 \mathbf{B}^{-2} \\ \vdots \\ \frac{1}{K} \text{tr} p_{L-1}^{\frac{1}{2}} \mathbf{D}_{L-1} \mathbf{B}^{-2} \end{bmatrix} \quad (14)$$

with $\mathbf{A} \in \mathbb{R}^{L \times L}$, $[\mathbf{A}]_{l,l'} = \frac{1}{K} p_l^{\frac{1}{2}} \text{tr} \mathbf{D}_l \mathbf{B}^{-2} p_{l'}^{\frac{1}{2}} \mathbf{D}_{l'}$, $\mathbf{B} = \sum_{l=0}^{L-1} \frac{1}{M_l} \sum_{m=0}^{M_l-1} \frac{\xi_{l,m}}{1 + c_l \xi_{l,m} b_l} p_l^{\frac{1}{2}} \mathbf{D}_l$, and $\mathbf{D}_{l'} = \frac{1}{M_{l'}} \sum_{m=0}^{M_{l'}-1} \frac{c_{l'} \xi_{l',m}^2}{(1 + c_{l'} \xi_{l',m} b_{l'})^2} \mathbf{D}_{l'}$. We now have all the ingredients to express the deterministic equivalent of the individual transmit powers at the APs.

Theorem 1. Under (As1) – (As4), for a fixed L and considering the channel model in (3), we have $(p_l - \bar{p}_l) \xrightarrow{\text{a.s.}} 0$, where

$$\bar{p}_l = \frac{1}{M_l^2} \text{tr} \mathbf{D}_{\text{sel},l} \mathbf{D}_p^{\frac{1}{2}} \mathbf{V} \quad (15)$$

$$\mathbf{V} = \text{blkdiag} \left(\left\{ (\mathbf{I}_{M_l} + c_l b_l \mathbf{C}_{\text{AP},l})^{-2} c_l b_l \mathbf{C}_{\text{AP},l} \right\}_{l=0}^{L-1} \right) \quad (16)$$

and $\mathbf{D}_{\text{sel},l} = \text{blkdiag} \left(\left\{ \delta_{l,l'} \mathbf{I}_{M_{l'}} \right\}_{l'=0}^{L-1} \right)$, where $\delta_{l,l'}$ is the Kronecker delta function, selects the antenna indexes of the AP l .

Proof. Based on [14, Th. 1], it is omitted due to lack of space. \square

Eq. (15) is a fixed-point equation in the APs powers and can be solved by using standard fixed-point methods (e.g., [6, Algorithm 1]). The variables $\{b_l\}$ can also be computed via fixed-point algorithm, while $\{\bar{b}_l\}$ are computed in closed form as a function of $\{b_l\}$. Note that the computation of $\{\bar{p}_l\}$ requires knowing only the second-order channel statistics (i.e., LSF and correlation coefficients), which are much more stable over time. The CU, in our proposed strategy, performs the following steps:

1. Receive the updated LSF coefficients from all the L APs.
2. Compute $\{\bar{p}_l\}$ by solving (15) $\forall l \in \{0, \dots, L-1\}$.
3. Select the active APs, $\mathcal{L}_a^* = \{l \in \{0, \dots, L-1\} \mid \bar{p}_l > \epsilon\}$.¹
4. For the whole time interval where the LSF remains constant, receive from the APs in \mathcal{L}_a^* the updated instantaneous channel coefficients, whose number is reduced to $\sum_{l \in \mathcal{L}_a^*} M_l K Q$, and compute the precoding matrices via (10). Then, send the precoding coefficients to the APs in \mathcal{L}_a^* .

5. PERFORMANCE EVALUATION

In the numerical simulations, we assume a square deployment area of 1×1 km² with 16 possible AP locations on a regular grid, where the positions of the L APs are randomly selected at every channel realization. The users are uniformly distributed within the scenario, with a minimum distance of 10 m to an AP, and their locations are randomly generated at every channel realization. We consider a constant number of antennas per AP, set to $M = 8$. When characterizing the average gains in power consumption, we consider a number of users varying from $K = 1$ to $K = 19$, as well as a number of APs ranging from $L = 2$ to $L = 10$. The target SNRs $\{\gamma_k\}$ are randomly generated between 1 dB and 20 dB with a uniform distribution, while the noise power is $10 \log_{10}(\sigma_\nu^2) + 30 = -96$ dBm. The LSF coefficients are computed (in dB) as $10 \log_{10}(\beta_{k,l}) = -30.5 - 37.6 \log_{10} d_{k,l} + F_{k,l}$ [15], where $d_{k,l}$ is the distance (in meters) between the user k and the AP l , and $F_{k,l} \sim \mathcal{N}(0, 16)$ represents the shadow fading. The correlation between the antennas of an AP follows the exponential model, i.e., $[\mathbf{C}_{\text{AP},l}]_{m,m'} = \rho^{|m-m'|}$ [16], where we set $\rho = 0.7$. We consider a PA maximal transmit power and efficiency of $p_{\text{max}} = 3$ W and $\eta_{\text{max}} = 0.34$, respectively [17]. The fixed power consumption is set to $P_{\text{fix}} = 15$ W, while the circuit power consumption per antenna is set to $P_c = 0.7$ W [18].

5.1. Single Channel Realization

Fig. 2 shows the antenna powers for a single channel realization, $K = 8$ users, $L = 8$ APs and $Q = 256$ subcarriers. We observe that the powers among the antennas of an AP share similar values, with a certain variability that is likely due to the correlation among antennas. The first and last antennas, being the least correlated given that we are considering a uniform linear array, are allocated more power. The RMT-based solution uses a uniform power per AP, and this power approximates the average of the optimal solution among the M antennas of the AP. Fig. 2 indicates also that the results in Theorem 1, even though derived for $M, K \rightarrow \infty$, are accurate for finite and relatively low values of M and K .

It is interesting to notice how the solution that minimizes the PAs consumed power turns on/off entire APs. All the antennas of the active APs are utilized, and vice versa. Instead, the solution that optimizes transmit power always activates all the APs. The consumed

¹The value of ϵ is related to the performance of the fixed-point algorithm and can be set empirically.

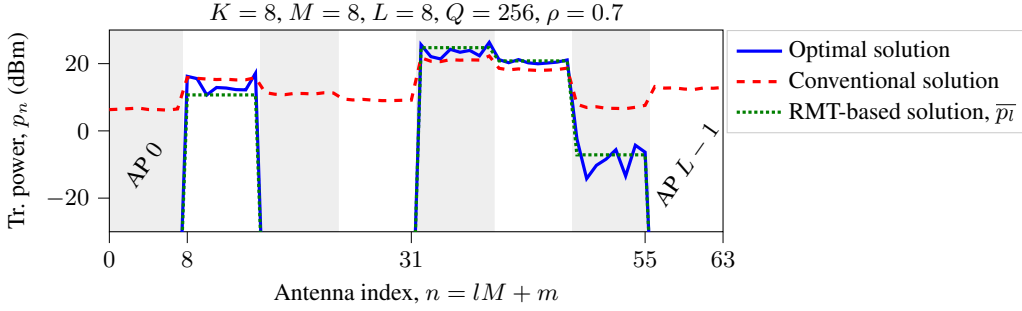


Fig. 2. Transmit power as a function of the antenna index for a single realization of a per-AP Kronecker channel. The graph shows the transmit power per antenna for: the optimal solution (10), the conventional one (8), and the one based on RMT (Theorem 1).

power solution utilizes $L_a = 4$ APs, corresponding to a halving in the fronthaul requirements. The gain in network consumption (i.e., the ratio between P_{net} by using the proposed solution and P_{net} by using the conventional solution), equals 1.78 both using the optimal solution and the RMT-based one, while the gains in PAs consumption are 1.28 and 1.27, respectively.

5.2. Impact of Number of Subcarriers

We observe, via numerical experiments, that the uniform power allocation per AP in (As2) approximates well the optimal solution when Q grows. This is in line with the findings in [6] for cellular systems, where uniform allocation among all the BS antennas is optimal (in terms of PAs consumption) when Q is large and there is no spatial correlation. Fig. 3 depicts the ratio between the values of P_{PAs} by using the optimal (11) and asymptotic (15) transmit powers as a function of Q . For a few subcarriers, the optimal solution activates only a part of the antennas of certain APs. When Q is sufficiently large, instead, the two strategies achieve the same performance. This tells us that the essential information is given by the set \mathcal{L}_a^* . Once we know which APs to activate, we can use a uniform power allocation among them with a negligible performance loss.

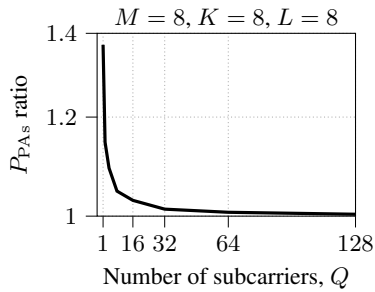


Fig. 3. Ratio between PA consumption by using the asymptotic solution and the optimal one as a function of the number of subcarriers, averaged over 10^2 channel realizations.

5.3. Achievable Gains in Network Consumption

Fig. 4 illustrates the average achievable savings in network consumption by using the asymptotic solution $\{\bar{p}_i\}$ over the conventional one for $Q = 256$ subcarriers. As expected, the more the APs, the larger the gains, as the consumed power solution activates only a fraction

of the L APs in low and medium loads. The savings decrease as K increases because (i) more users require the activation of more antennas and (ii) it is more likely that a user will be in the proximity of each AP. For $L = 10$ APs, the gain reaches a factor of $9\times$ when there is $K = 1$ user and remains large also for $K = 7$, when it equals 2. For $L = 8$ APs and $K = 9$ users, the saving is still equal to 1.5 (corresponding to a 50% less consumed power). In general, the ratios become lower or equal than 1.5 when $K > L$.

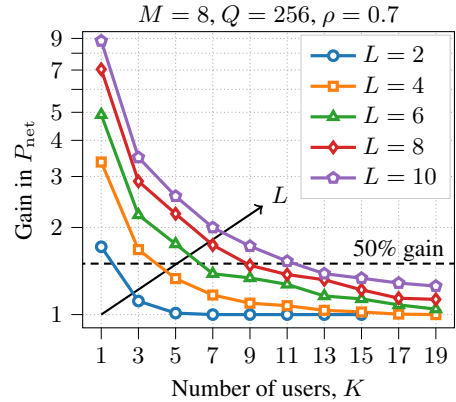


Fig. 4. Gain in network power consumption (of utilizing the RMT-based solution against the conventional one), averaged over 10^2 channel realizations, as a function of the number of users for different number of APs, $M = 8$ antennas, and $Q = 256$ subcarriers.

6. CONCLUSION

The problem of designing CF-mMIMO precoders that minimize the PAs consumption subject to rate constraints with centralized processing has been addressed. Under a per-AP Kronecker channel model, we applied RMT to derive simple fixed-point equations in the antenna powers that depend only on the channel covariances and are accurate when the number of subcarriers grows. The optimal strategy consists of activating all the antennas of certain APs with uniform powers and deactivating all the antennas of the remaining APs. By switching off the circuits of the non-active APs, we achieved significant savings in the network power consumption in low and medium loads. Perspectives include the consideration of local processing (i.e., performed at the individual APs) and the analysis of user-centric implementations.

7. REFERENCES

- [1] S. Zhang, S. Xu, G.Y. Li, and E. Ayanoglu, “First 20 years of green radios,” *IEEE Trans. Green Commun. Netw.*, vol. 4, no. 1, pp. 1–15, 2020.
- [2] T. Islam, D. Lee, and S.S. Lim, “Enabling network power savings in 5G-advanced and beyond,” *IEEE J. Sel. Areas Commun.*, vol. 41, no. 6, pp. 1888–1899, 2023.
- [3] S. Wesemann, J. Du, and H. Viswanathan, “Energy efficient extreme MIMO: Design goals and directions,” *IEEE Commun. Mag.*, pp. 1–7, 2023.
- [4] H.V. Cheng, D. Persson, and E.G. Larsson, “Optimal MIMO precoding under a constraint on the amplifier power consumption,” *IEEE Trans. Commun.*, vol. 67, no. 1, pp. 218–229, 2019.
- [5] K. Senel, E. Björnson, and E.G. Larsson, “Joint transmit and circuit power minimization in massive MIMO with downlink SINR constraints: When to turn on massive MIMO?,” *IEEE Trans. Wirel. Commun.*, vol. 18, no. 3, pp. 1834–1846, 2019.
- [6] E. Peschiera and F. Rottenberg, “Energy-saving precoder design for narrowband and wideband massive MIMO,” *IEEE Trans. Green Commun. Netw.*, 2023.
- [7] E. Nayebi, A. Ashikhmin, T.L. Marzetta, and H. Yang, “Cell-free massive MIMO systems,” in *Proc. 49th Asilomar Conf. Signals Syst. Comput.*, 2015, pp. 695–699.
- [8] C. Wang et al., “On the road to 6G: Visions, requirements, key technologies, and testbeds,” *IEEE Commun. Surveys Tuts.*, vol. 25, no. 2, pp. 905–974, 2023.
- [9] T. Van Chien, E. Björnson, and E.G. Larsson, “Joint power allocation and load balancing optimization for energy-efficient cell-free massive MIMO networks,” *IEEE Trans. Wirel. Commun.*, vol. 19, no. 10, pp. 6798–6812, 2020.
- [10] Q. He, Ö.T. Demir, and C. Cavdar, “Dynamic AP selection and cluster formation with minimal switching for green cell-free massive MIMO networks,” in *Proc. Joint Eur. Conf. Netw. Commun. 6G Summit*, 2023, pp. 234–239.
- [11] F. Kooshki, A.G. Armada, M.M. Mowla, A. Flizikowski, and S. Pietrzyk, “Energy-efficient sleep mode schemes for cell-less RAN in 5G and beyond 5G networks,” *IEEE Access*, vol. 11, pp. 1432–1444, 2023.
- [12] W. Weichselberger, M. Herdin, H. Ozelik, and E. Bonek, “A stochastic MIMO channel model with joint correlation of both link ends,” *IEEE Trans. Wireless Commun.*, vol. 5, no. 1, pp. 90–100, 2006.
- [13] R. Couillet and M. Debbah, *Random Matrix Methods for Wireless Communications*, Cambridge Univ. Press, New York, NY, USA, 2011.
- [14] R. Couillet, M. Debbah, and J.W. Silverstein, “A deterministic equivalent for the analysis of correlated MIMO multiple access channels,” *IEEE Trans. Inf. Theory*, vol. 57, no. 6, pp. 3493–3514, 2011.
- [15] 3GPP, *Further advancements for E-UTRA physical layer aspects (Release 9)*, 3GPP TS 36.814, Mar. 2017.
- [16] S.L. Loyka, “Channel capacity of MIMO architecture using the exponential correlation matrix,” *IEEE Commun. Lett.*, vol. 5, no. 9, pp. 369–371, 2001.
- [17] Qorvo QPA4501, *4.4 - 5.0 GHz, 3 Watt, 28 Volt GaN Power Amplifier Module*, 2021, Rev. C.
- [18] G. Auer et al., “How much energy is needed to run a wireless network?,” *IEEE Wireless Commun.*, vol. 18, no. 5, pp. 40–49, 2011.